HHS Public Access

Author manuscript

Science. Author manuscript; available in PMC 2022 January 10.

Published in final edited form as:

Science. 2020 September 25; 369(6511): 1633–1637. doi:10.1126/science.abb9818.

Succination inactivates gasdermin D and blocks pyroptosis

Fiachra Humphries[1], **Liraz Shmuel-Galia**[1], **Natalia Ketelut-Carneiro**[1], **Sheng Li**[2], **Bingwei Wang**[3], **Venkatesh V. Nemmara**[4], **Ruth Wilson**[1], **Zhaozhao Jiang**[1], **Farnaz Khalighinejad**[5], **Khaja Muneeruddin**[6,7], **Scott A. Shaffer**[6,7], **Ranjan Dutta**[8], **Carolina Ionete**[5], **Scott Pesiridis**[9], **Shuo Yang**[2], **Paul R. Thompson**[7], **Katherine A. Fitzgerald**[1,*]

[1]Program in Innate Immunity, Department of Medicine, University of Massachusetts Medical School, Worcester, MA 01605, USA.

[2]Department of Immunology, Key Laboratory of Immunological Environment and Disease, State Key Laboratory of Reproductive Medicine, Nanjing Medical University, Nanjing, China.

[3]Department of Pharmacology, Nanjing University of Chinese Medicine, Nanjing, China.

[4]Department of Chemistry and Biochemistry, Rowan University, Glassboro, NJ 08028, USA.

[5]Department of Neurology, University of Massachusetts Medical School, Worcester, MA 01605, USA.

[6]Mass Spectrometry Facility, University of Massachusetts Medical School, Shrewsbury, MA 01545, USA.

[7]Department of Biochemistry and Molecular Pharmacology, University of Massachusetts Medical School, Worcester, MA 01605, USA.

[8]Department of Neurosciences, Lerner Research Institute, Cleveland Clinic, Case Western Reserve University, Cleveland, OH 44106, USA.

[9]Innate Immunity Research Unit, GlaxoSmithKline, Collegeville, PA 19426, USA.

Abstract

Activated macrophages undergo a metabolic switch to aerobic glycolysis, accumulating Krebs' cycle intermediates that alter transcription of immune response genes. We extended these observations by defining fumarate as an inhibitor of pyroptotic cell death. We found that dimethyl

[*]**Corresponding author**. kate.fitzgerald@umassmed.edu.

Author contributions: F.H. conceived the study, developed the concept, performed experiments, analyzed data, and wrote the manuscript. L.S.-G., N.K.-C., R.W., and Z.J. performed experiments and analyzed data. S.L., B.W., and S.Y. performed and analyzed EAE experiments. S.P. provided experimental advice. C.I., R.D., and F.K. provided clinical expertise and PBMCs from consenting MS patients through the University of Massachussetts MS Center biorepository. S.A.S. and K.M. designed and performed mass spectrometry experiments. V.V.M. and P.R.T. synthesized the MMF-Yne probe. K.A.F. conceived the study, developed the concept, supervised the research, and wrote the manuscript.

Competing interests: K.A.F. serves on the scientific advisory board of Quench Bio and NodThera. The University of Massachusetts Medical School have filed a provisional patent application on succination of GSDMD described in this study, listing F.H., P.T., and K.A.F. as inventors.

Data and materials availability: All data in this paper are presented in the main text and supplementary materials.

SUPPLEMENTARY MATERIALS

science.sciencemag.org/content/369/6511/1633/suppl/DC1

fumarate (DMF) delivered to cells or endogenous fumarate reacts with gasdermin D (GSDMD) at critical cysteine residues to form S-(2-succinyl)-cysteine. GSDMD succination prevents its interaction with caspases, limiting its processing, oligomerization, and capacity to induce cell death. In mice, the administration of DMF protects against lipopolysaccharide shock and alleviates familial Mediterranean fever and experimental autoimmune encephalitis by targeting GSDMD. Collectively, these findings identify GSDMD as a target of fumarate and reveal a mechanism of action for fumarate-based therapeutics that include DMF, for the treatment of multiple sclerosis.

Cell death pathways are important for host defense. Necroptosis and pyroptosis also contribute to inflammatory disease through the release of danger-associated molecular patterns (DAMPs) (1). The pore-forming protein gasdermin D (GSDMD) is the executioner of pyroptosis. Caspase cleavage of GSDMD liberates an N-terminal p30 fragment (GSDMD-N), which oligomerizes and forms pores in the plasma membrane. These pores serve as a conduit for the release of interleukin-1β (IL-1β) and IL-18 and, ultimately, the demise of the cell (1, 2).

Numerous studies have shown that cell metabolism affects inflammatory responses. Lipopolysaccharide (LPS)–activated macrophages switch from oxidative phosphorylation to aerobic glycolysis. Krebs' cycle intermediates, such as succinate and itaconate, accumulate and moonlight as positive and negative regulators of inflammatory gene expression (3-8). To determine whether Krebs' cycle intermediates modulate pyroptosis, we tested their effect on inflammasome responses. Bone marrow–derived macrophages (BMDMs) were primed with LPS for 2 hours before being exposed to metabolites and then exposed to nigericin (Nig). Inflammasome activation and pyroptosis were then measured. The metabolites were added after LPS to avoid any impact on transcription. Dimethyl fumarate (DMF) potently blocked LPS-Nig–induced release of lactate dehydrogenase (LDH) (Fig. 1A) and IL-1β (Fig. 1B) but not tumor necrosis factor–α (TNF-α) (Fig. 1C). DMF also blocked the formation of GSDMD-N (Fig. 1D). Monomethyl fumarate (MMF), a cell-impermeable derivative of fumarate, had no inhibitory effect. DMF impaired kinetic cell death over 6 hours (Fig. 1E and fig. S1A). DMF even impaired cell death when added after Nig treatment (fig. S1, B and C). The inhibitory effect of DMF was also observed in BMDMs after transfected LPS (Fig. 1F), Salmonella infection (fig. S1, D and E), or poly(deoxyadenylic-thymidylic) [poly(dA:dT)] (fig. S1, F and G). DMF also blocked LPS-Nig–induced cell death and LDH release in human THP1 (fig. S2, A to C) and $CD14^+$ monocytes (fig. S2, D and E). BMDMs pretreated with DMF had decreased GSDMD oligomerization in response to LPS-Nig, indicating that DMF blocks pore formation (Fig. 1G).

Fumarate accumulated in LPS-activated macrophages (fig. S2F), similar to prior studies (5, 7). To assess the effect of endogenous fumarate, we induced its accumulation in cells by blocking fumarate hydratase with FHIN1 (Fig. S2F). FHIN1 impaired cell death (Fig. 1H and fig. S2G) and reduced the formation of GSDMD-N (Fig. 1I). DMF has previously been reported to exhibit antiinflammatory activity through nuclear respiratory factor 2 (NRF2) or glyceraldehyde-3-phosphate dehydrogenase (GAPDH) (9, 10). Cells treated with the GAPDH inhibitor heptilidic acid (HA) (11) or the NRF2 inhibitor ML385 (12) had no impact on cell death (fig. S3, A and B), LDH release (fig. S3C), IL-1β release (fig. S3D), or

GSDMD-N formation (fig. S3, E and F). HA and ML385 inhibited the GAPDH and NRF2 target genes *Nos2* and *Hmox1*, respectively (fig. S3, G to I). Suppression by means of small interfering RNA of the gene encoding NRF2 (*Nfe2l2*) also failed to affect pyroptosis (fig. S3, J an K). Thus, the regulatory effects of DMF are independent of NRF2 or GAPDH. Fumarate also suppressed pyroptosis in vivo. Wild-type (WT) mice receiving a lethal dose of LPS succumbed to LPS shock within 48 hours, whereas mice administered LPS and a single dose of DMF showed increased survival (Fig. 1J). DMF reduced IL-1β (Fig. 1K) but not TNF-α levels (Fig. 1L). An in vivo–compatible fumarate hydratase inhibitor, FHIN2, that elevated fumarate levels in vivo also reduced IL-1β levels (fig. S4, A and B). Thus, fumarate inhibits pyroptosis in vivo.

We next used a chemoproteomic approach to identify targets of DMF. We synthesized monomethyl fumarate alkyne (MMF-Yne), a cell-permeable fumaric acid–alkyne (13) that mimics DMF but has an alkyne handle, for target identification (fig. S5, A and B). Like DMF, MMF-Yne inhibited LPS-Nig–induced LDH release (fig. S5C) and IL-1β (fig. S5D). To identify MMF-Yne–bound targets, we used click chemistry (fig. S6). Immunoblotting revealed that the probe reacts with multiple proteins in pyroptotic lysates (fig. S7A). Treatment with unlabeled DMF reduced the MMF-Yne signal (fig. S7A). Mass spectrometry identified GSDMD as a MMF-Yne target (fig. S7B). MMF-Yne dose-dependently labeled GSDMD (Fig. 2A). Furthermore, DMF blocked MMF-Yne labeling of GSDMD (Fig. 2B). Maximum occupancy of 1 μM GSDMD was achieved at 25 μM DMF (fig. S7, C to E). Thus, DMF can target GSDMD.

Fumarate derivatizes protein cysteines to generate 2-(succinyl)-cysteine, an irreversible posttranslational modification that affects protein function (9). Liquid chromatography–tandem mass spectrometry (LCMS/MS) peptide mapping experiments showed that treatment of recombinant human or mouse GSDMD with MMF led to abundant monomethyl succination (2-monomethyl succinyl-cysteine) at Cys^{191} in human and Cys^{192} in mouse GSDMD, respectively (fig. S8, A and C). DMF also modified (2-dimethyl succinyl-cysteine) GSDMD at the same cysteines (fig. S8, B and D). Neither of these were detected in vehicle controls. In addition to Cys^{192}, mouse GSDMD was succinated on nine other cysteines (table S1). Human GSDMD was succinated on four additional cysteines (table S1). We also immunoprecipitated GSDMD from DMF-treated BMDMs and analyzed tryptic digests by means of MS/MS. This approach revealed a combination of 2-monomethyl and 2-dimethyl succination of GSDMD on Cys^{192} (Fig. 2, C and D) as well as Cys^{57} and Cys^{77} (fig. S9). LPS-Nig treatment in the presence of FHIN1 also resulted in modification of GSDMD by endogenous fumarate (fig. S10, A and B). Thus, GSDMD is succinated by exogenous or endogenous fumarate.

Cys^{192} (Cys^{191} in humans) is critical for GSDMD-N oligomerization (14). MMF-Yne modifies full-length GSDMD and GSDMD-N but not GSDMD-N-C192A (Fig. 2E). Although GSDMD-N induced cell permeability and LDH release in human embryonic kidney (HEK) 293T cells, which is consistent with previous studies (14, 15), GSDMD-N-C192A did not (Fig. 2, F and G). DMF inhibited the GSDMD-N–induced release of LDH (Fig. 2H). Because DMF can impair both processing and activity of GSDMD, we hypothesized that succination may prevent caspase 1–GSDMD interactions. DMF

completely blocked this (Fig. 2I). Processing of caspase 1 was not impaired by DMF. Succination of GSDMD in vitro also reduced its binding to caspase 1 that was immunoprecipitated from cells (Fig. 2J). Thus, DMF modifies GSDMD, blocking its processing, oligomerization, and cell death.

GSDMD is critical for pyroptosis. However, in its absence, cell death still occurs, albeit with slower kinetics (2). Consistently, DMF inhibited cell death in both WT and *Gsdmd*-deficient BMDMs (Fig. 3A) and THP1 cells (Fig. 3B). DMF similarly suppressed LDH (Fig. 3C) and IL-1β levels in both WT and *Gsdmd*-deficient BMDMs (Fig. 3D). Gasdermin E (GSDME) drives apoptosis in *GSDMD*-deficient cells (16). GSDME processing in *Gsdmd*-deficient cells was also blocked by DMF (Fig. 3E). DMF inhibited GSDMD- and GSDME-driven cell death comparably (fig. S11, A and B). MMF-Yne also modifies GSDME (Fig. 3F). DMF and MMF succinated GSDME at Cys^{45} (Fig. 3, G and H) and additional sites (table S1). Treatment of cells with FHIN1 attenuated GSDMD-independent (GSDME-dependent) cell death (Fig. 3I) and the generation of GSDME-N (Fig. 3J). Thus, fumarate modifies GSDMD and GSDME through succination.

GSDMD is an important driver of inflammatory diseases (17). *Gsdmd*-deficient mice are protected from experimental autoimmune encephalitis (EAE) (18). Fumarate analogs such as DMF are approved by the U.S. Food and Drug Administration (FDA) for the treatment of multiple sclerosis (MS). Two newer MS drugs, diroximel fumarate and tepilamide fumarate, also blocked LPS-Nig–induced pyroptosis and GSDMD-N formation (fig. S12, A to C). DMF blocked the onset of EAE and reduced neuropathology and demyelination (Fig. 4, A to C). DMF also reduced GSDMD-N in central nervous system (CNS) tissue (Fig. 4, B and D). GSDMD was essential for cell infiltration to the CNS during EAE. Mice receiving DMF demonstrated reduced infiltration of myeloid cells, $CD4^+$ and $CD8^+$ T cells (Fig. 4, E and F, and fig. S13A). DMF reduced T helper 1 (T_H1) [interferon-γ^+ (IFN-γ^+)] and T_H17 (IL-$17A^+$) cell numbers in the CNS (Fig. 4, G and H, and fig. S13B). Post mortem brain tissue from MS patients stained positive for GSDMD-N (Fig. 4I and table S4). Patients with MS had elevated levels of IL-1β and GSDMD-N in peripheral blood mononuclear cells (PBMCs) (Fig. 4, J to L, and table S3). Both IL-1β and GSDMD-N were reduced in patients taking DMF (Tecfidera) (Fig. 4, J to L, and table S3). Thus, DMF reduces GSDMD-driven responses in EAE, which supports a model in which elevated GSDMD contributes to MS. GSDMD has also been linked to familial Mediterranean fever (FMF). FMF results from constitutive activation of the pyrin inflammasome, and mice that harbor the $Mefv^{V726/726}$ allele exhibit features of the human disease. *Gsdmd*-deficient mice are rescued from disease in this model (19). Administration of DMF alleviated weight loss, splenomegaly, IL-1β secretion, GSDMD-N formation, and liver pathology in the $Mefv^{V726/V726}$ mouse model (fig. S14, A to E).

These data collectively indicate that fumarate mitigates pyroptosis. Succination of GSDMD on Cys^{192} prevents its processing and oligomerization, which limits pore formation, cytokine release, and cell death (fig. S15). Additional studies reinforce the importance of Cys^{191}/Cys^{192} as a target of other GSDMD-targeting drugs (15, 20, 21). Our study provides mechanistic insight into the immunomodulatory activity of Tecfidera (DMF) used for MS and underscores the importance of GSDMD as a driver of chronic inflammation. This

work also highlights the potential for the treatment of chronic inflammatory diseases with inhibitors of GSDMD.

Supplementary Material

Refer to Web version on PubMed Central for supplementary material.

Funding:

This work is supported by pilot grants from the Worcester Foundation for Biomedical Research and the Dan and Diane Riccio Fund for Neuroscience from UMASS Medical School. F.H. is a GSK postdoctoral fellow. N.K.-C. is a Cancer Research Irvington Fellow, and L.S.-G. is an EMBO long-term fellow and a Crohn's and Colitis Foundation fellow.

REFERENCES AND NOTES

1. Shi J et al., Nature 526, 660–665 (2015). [PubMed: 26375003]
2. Kayagaki N et al., Nature 526, 666–671 (2015). [PubMed: 26375259]
3. Mills EL et al., Nature 556,113–117 (2018). [PubMed: 29590092]
4. Liao S-T et al., Nat. Commun 10, 5091 (2019). [PubMed: 31704924]
5. Lampropoulou V et al. Cell Metab. 24, 158–166 (2016). [PubMed: 27374498]
6. Bambouskova M et al., Nature 556, 501–504 (2018). [PubMed: 29670287]
7. Tannahill GM et al., Nature 496, 238–242 (2013). [PubMed: 23535595]
8. Muhammad JS et al., ImmunoTargets Ther. 8, 29–41 (2019). [PubMed: 31687364]
9. Blatnik M, Frizzell N, Thorpe SR, Baynes JW, Diabetes 57, 41–49 (2008). [PubMed: 17934141]
10. Kornberg MD et al., Science 360, 449–453 (2018). [PubMed: 29599194]
11. Singh A et al., ACS Chem. Biol 11, 3214–3225 (2016). [PubMed: 27552339]
12. Kato M, Sakai K, Endo A, Biochim. Biophys. Acta 1120, 113–116 (1992). [PubMed: 1554737]
13. Kulkarni RA et al., Nat. Chem. Biol 15, 391–400 (2019). [PubMed: 30718813]
14. Liu X et al., Nature 535, 153–158 (2016). [PubMed: 27383986]
15. Hu JJ et al., Nat. Immunol 21, 736–745 (2020). [PubMed: 32367036]
16. Rogers C et al., Nat. Commun 10, 1689 (2019). [PubMed: 30976076]
17. McKenzie BA et al., Proc. Natl. Acad. Sci. U.S.A 115, E6065–E6074 (2018). [PubMed: 29895691]
18. Li S et al., J. Exp. Med 216, 2562–2581 (2019). [PubMed: 31467036]
19. Kanneganti A et al., J. Exp. Med 215, 1519–1529 (2018). [PubMed: 29793924]
20. Rathkey JK et al., Sci. Immunol 3, eaat2738 (2018). [PubMed: 30143556]
21. Sollberger G et al., Sci. Immunol 3, eaar6689 (2018). [PubMed: 30143555]

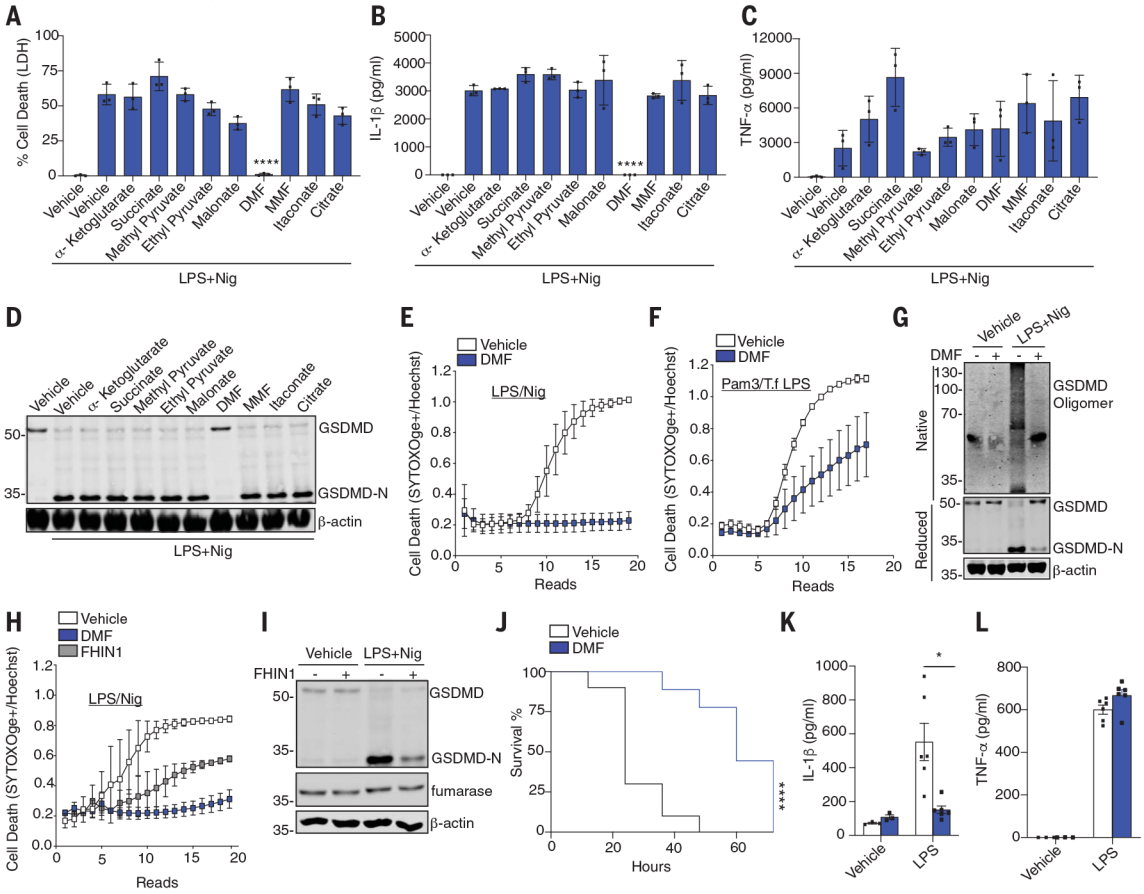

Fig. 1. DMF inhibits pyroptosis.

(**A** to **F**) BMDM treated as indicated and LDH, IL-1β, or TNF-α measured with [(A) to (C)] enzyme-linked immunosorbent assay (ELISA), (D) GSDMD/β-actin by immunoblotting, or [(E) and (F)] permeability of cells to SYTOX Orange. (**G**) GSDMD oligomerization in native and reduced cell lysates treated as above. (**H** and **I**) Time course of permeabilization to SYTOX Orange or GSDMD-N formation in cells treated as indicated. (**J**) Survival rates of WT mice after 50 mg/kg of LPS ($n = 10$ mice) or LPS$^+$ DMF ($n = 9$ mice). (**K** and **L**) Serum IL-1β or TNF-α levels of WT mice 5 hours after intraperitoneal injection with 5 mg/kg LPS ($n = 6$ mice) or phosphate-buffered saline (PBS) ($n = 3$ mice). (A) to (C) are pooled from three independent experiments. (D) to (I) are representative from three independent experiments. In (J) to (L), data points indicate individual mice. *$P < 0.05$; **$P < 0.01$; ***$P < 0.001$; ****$P < 0.0001$) [(J), Mantel–Cox survival analysis; (A) to (C) and (K), two-way analysis of variance (ANOVA)]. Error bars indicate means ± SEM.

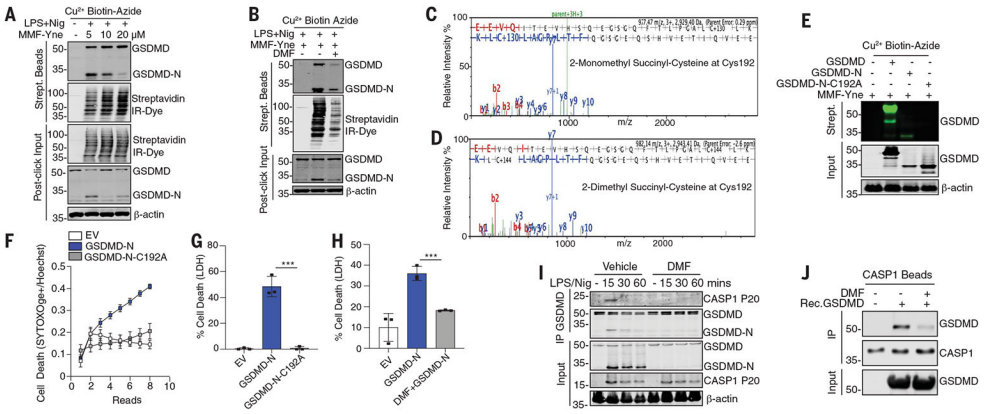

Fig. 2. Succination of GSDMD inhibits pyroptosis.

(**A** and **B**) Immunoblot of GSDMD in streptavidin pulldown from clicked lysates treated as indicated. (**C** and **D**) Representative mass spectrometry spectra of 2-monomethyl and 2-dimethylsuccination of GSDMD immunoprecipitated from DMF-treated BMDMs. (**E**) Immunoblot of GSDMD in clicked lysates from transfected HEK293T cells. (**F** to **H**) Cell death of HEK293T transfected as indicated. (**I**) Immunoblots of CASP1p20 and GSDMD in BMDMs. (**J**) Immunoblots of an in vitro binding assay of succinated and nonsuccinated GSDMD incubated with caspase 1 beads. [(A), (B), (F), (J), and (K)] Representative images from three independent experiments. [(C) to (E)] Representative mass spectrometry spectra from two independent experiments. [(H) and (I)] Pooled data from three independent experiments. ***$P < 0.001$ (one-way ANOVA). Error bars indicate means ± SEM.

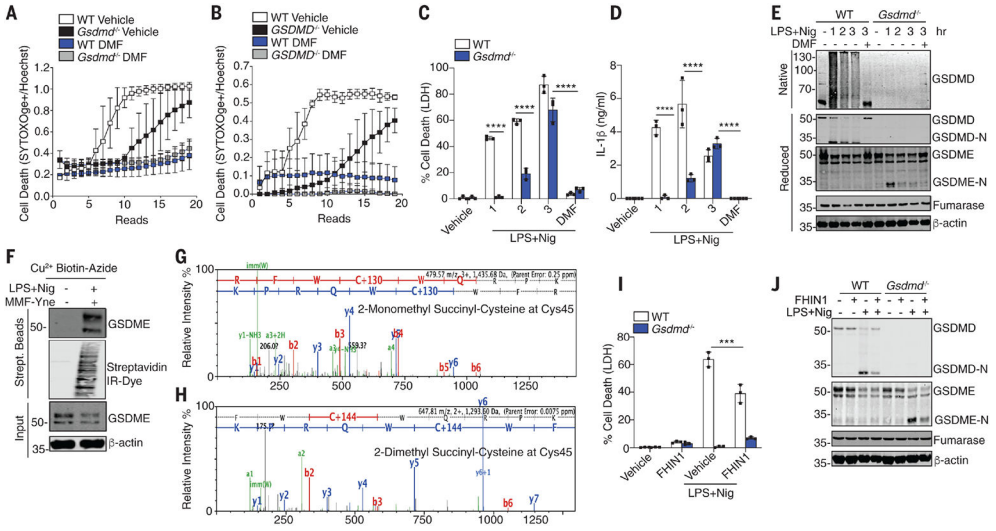

Fig. 3. DMF targets GSDMD and GSDME.

(**A** and **B**) Kinetic cell death of (A) WT and *Gsdmd*$^{-/-}$ BMDMs or (B) WT and *GSDMD*$^{-/-}$ THP1 cells treated as indicated. (**C** and **D**) LDH and IL-1β release from WT and *Gsdmd*$^{-/-}$ BMDMs. (**E**) Immunoblot of GSDMD and GSDME in native and reduced cell lysates from BMDMs. (**F**) Immunoblot of GSDME in streptavidin pulldown from clicked lysates. (**G** and **H**) Representative mass spectrometry spectra of succinated GSDME. (**I**) Immunoblot analysis of GSDMD and GSDME from WT and *Gsdmd*$^{-/-}$ BMDMs. [(A) and (B)] Representative of three independent experiments. [(C), (D), and (I)] Pooled data from three independent experiments. [(E), (F), and (J)] Representative images from three independent experiments. ***$P < 0.0001$; ****$P < 0.00001$ (two-way ANOVA). Error bars indicate means ± SEM.

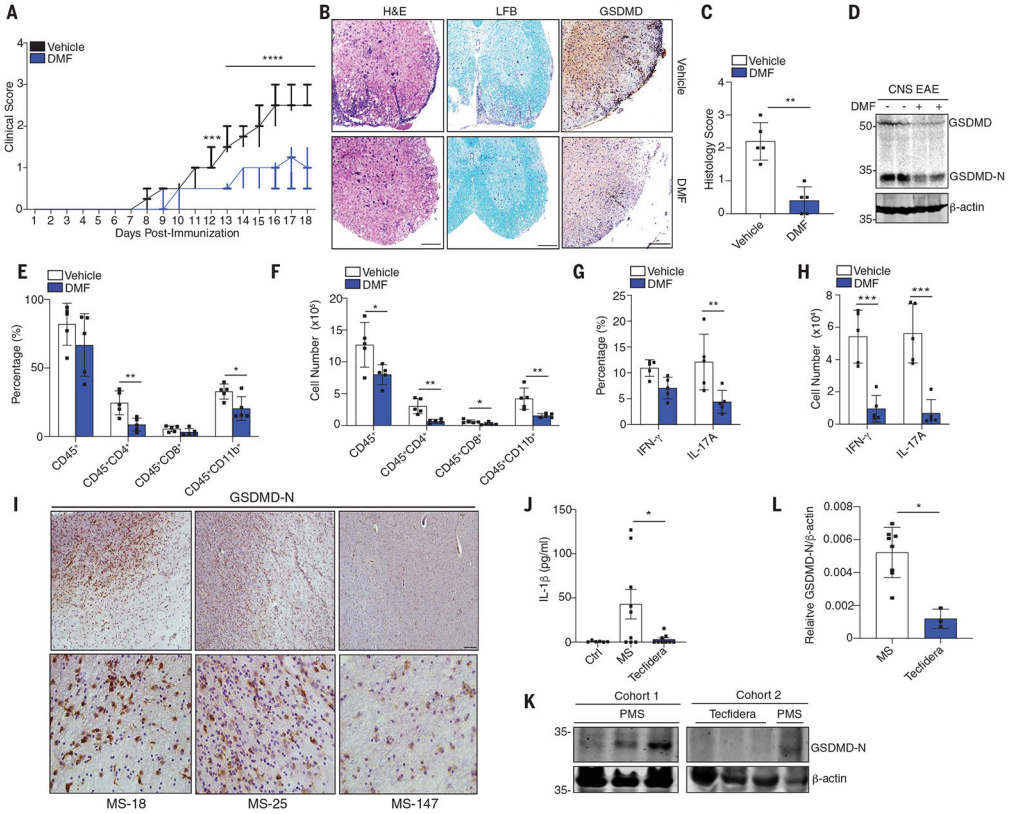

Fig. 4. Succination of GSDMD alleviates EAE and MS.

(**A**) Clinical scores of WT mice administered vehicle or DMF daily after EAE induction, respectively ($n = 10$ mice). (**B**) Representative hematoxylin and eosin (H&E), Luxol fast blue (LFB), and anti-GSDMD staining and (**C**) pathology evaluation of spinal cord sections from mice, showing inflammatory cell infiltration and demyelination, respectively. Scale bar, 200 μm. (**D**) Immunoblot of GSDMD in spinal cord tissue. (**E** and **F**) Flow cytometry analysis of $CD45^+$ leukocytes, $CD45^+CD4^+$ T cells, $CD45^+CD8^+$ T cells, and $CD45^+CD11b^+$ monocytes that infiltrated the spinal cords and brains of the mice in (A) ($n = 5$ mice). (**G** and **H**) T_H1 (IFN-γ^+) and T_H17 (IL-$17A^+$) cells from $CD4^+$ T cells ($n = 5$ mice). (**I**) Immunohistochemistry staining of GSDMD-N in post mortem lesions from MS patients. Scale bars, 100 μm (top), 25 μm (bottom). (**J**) IL-1β levels in serum from healthy controls ($n = 6$ donors), MS patients (MS; $n = 9$ donors), and MS patients receiving Tecfidera delayed release capsules ($n = 9$ donors). (**K**) Immunoblot of GSDMD-N and (L) densitometry analysis of GSDMD-N in PBMCs from [(J) and (K)] MS ($n = 8$ donors) or PMS Tecfidera ($n = 3$ donors). [(A), (C), and (E) to (H)] Pooled data from two independent EAE experiments. $^*P < 0.05$; $^{**}P < 0.01$; $^{***}P < 0.001$ [(A) and (C), Mann–Whitney U test; (E) to (H), multiple t test]. (A) Box and whisker plot. [(C), (E) to (H), (J), and (L)] Error bars indicate means ± SEM.